Journal of Molecular Catalysis A: Chemical 385 (2014) 78–84

Contents lists available at ScienceDirect

Journal of Molecular Catalysis A: Chemical

journal homepage: www.elsevier.com/locate/molcata

SPIONs-bis(NHC)-palladium(II): A novel, powerful and efficient catalyst for Mizoroki–Heck and Suzuki–Miyaura C–C coupling reactions

Marzieh Ghotbinejad, Ahmad R. Khosropour*, Iraj Mohammadpoor-Baltork*, Majid Moghadam, Shahram Tangestaninejad, Valiollah Mirkhani

Catalysis Division, Department of Chemistry, University of Isfahan, Isfahan 81746-73441, Iran

ARTICLE INFO

Article history:
Received 20 July 2013
Received in revised form
17 December 2013
Accepted 1 January 2014
Available online 8 January 2014

Keywords:
Mizoroki–Heck reaction
Suzuki–Miyaura reaction
SPIONs
TCT
N-Heterocyclic carbenes

ABSTRACT

A novel, stable and powerful nano Pd-NHC complex utilizing *N*-methylimidazole bounded to 1,3,5-triazine-tethered SPIONs (superparamagnetic iron oxide nanoparticles) as a bidentate NHC ligand is reported. This well-defined complex was used as an efficient (NHC)-based catalyst for Mizoroki–Heck and Suzuki–Miyaura cross coupling reactions. These cross coupled products were produced in excellent yields under conventional heating or microwave irradiation at extremely low palladium loading (~0.002 mol%) with perfect high turnover frequencies (TOFs) (10^3–10^6 h^{-1}). Moreover, the catalyst could be quickly and completely recovered by external magnetic field and be reused for seven reaction cycles without any change in catalytic activity.

1. Introduction

Recently, *N*-heterocyclic carbenes (NHCs) have emerged as an extremely useful and versatile class of ligands in homogeneous transition metal catalysis due to the strong σ-donor properties, ease of preparation and effective binding ability to any transition metal irrespective of their oxidation states [1–6]. Within this context, these compounds have attracted increasing attention in both academic and industrial fields owing to their unique catalytic activity [2,7]. NHCs complexes as homogeneous catalysts have been used in a number of organic transformations such as olefin metathesis, and C–C and C–N bond formation reactions [8]. In this regard, the discovery of catalytic properties of Pd-NHCs complexes in the Mizoroki–Heck and Suzuki–Miyaura cross-coupling reactions are considered as particularly useful since these reactions provide many vast applications in the synthesis of natural products, numerous drugs and high performance modern organic materials [9–14]. Despite the wide application of these homogeneous catalysts in organic transformations, their recycling is almost complicated and their separation is very difficult. Moreover, in consequence of toxicity of palladium residuals, acceptable limits of palladium traces in pharmaceuticals were set usually as ppm level. So, one way to overcome these drawbacks is immobilization of Pd-NHC on different solid supports [15–19]. For instance, the immobilization of Pd-NHCs complexes on polystyrene [20] or silica [21,22] has been reported. Meanwhile, utilizing of nano-supports in this case has attracted considerable interest due to their high activity and environmental acceptability [23]. Although, these materials offer high specific surface area of the active component which enhances the contact between reactants and supported catalyst, they are easily agglomerated and difficult separated. Moreover, due to specific nature of the mechanisms of Suzuki and Heck reactions, leaching of palladium from the support to the reaction mixture is the other problem [24]. This was a reason for the observed decrease in activity of recycled catalysts. So, even though the widespread Pd-NHC catalytic systems described previously, it is essential to design a more efficient, stable and easily recoverable palladium catalyst for C–C coupling reactions.

Currently, magnetic separation provides a very useful approach for removing magnetic nanoparticles (MNPs) with an external magnet. Meanwhile, various Pd-NHC immobilized on MNPs employing the property of magnetic separation have been developed in a number of C–C coupling reactions [25]. These magnetic nanoparticles show excellent catalytic activities. The magnetic separation method presents many advantages over conventional ones. This can be considered as an environmentally benign that the consequence caused by filtration steps was omitted in the reaction.

* Corresponding authors. Tel.: +98 311 7932715; fax: +98 311 6689732.
E-mail addresses: Khosropour@chem.ui.ac.ir (A.R. Khosropour), imbaltork@sci.ui.ac.ir (I. Mohammadpoor-Baltork).

1381-1169/$ – see front matter © 2014 Elsevier B.V. All rights reserved.
http://dx.doi.org/10.1016/j.molcata.2014.01.001

To date there are only a few examples of Pd-NHC anchored to MNPs with the catalytic behavior in the organic transformations [26]. Moreover, based on the character of reactants, temperature and catalyst activity of Pd-NHC immobilized on MNPs, the Suzuki–Miyaura or Mizoroki–Heck have been performed efficiently at 0.5–72 h using 1–10 mol% of palladium as active site of the catalyst system [27]. Consequently, there is a demand for the development of new Pd-NHC-MNPs with superior catalytic activities, less palliative and high recyclability. Encourage to our previous work on C–C-coupling reactions [28a] and also on imidazolium-tagged box ligands via synthesis of 1,3,5-triazine-functionalized bisimidazolium dichloride tethered to MNPs and their good performance and recyclability in Betti synthesis [28b], we designed and prepared SPIONs-bis(NHC)-palladium(II) (**4**) as a new and highly stable Pd-NHC-tagged MNPs and investigated their performance in the Mizoroki–Heck and Suzuki–Miyaura reactions.

2. Experimental

2.1. Materials

All chemicals were purchased from Merck chemical company. Fe_3O_4 nanoparticles and silica-coated magnetite nanoparticles (SiO_2@Fe_3O_4) were synthesized according to the literature [29]. All known organic products were identified by comparison of their physical and spectral data with those of authentic samples. Thin layer chromatography (TLC) was performed on UV-active aluminum-backed plates of silica gel (TLC Silica gel 60 F254).

2.2. Instrumentation and analysis

^{1}H and ^{13}C NMR spectra were recorded on a Bruker-avance 400 MHz spectrometer in $CDCl_3$. Coupling constants are given in Hz. The FT-IR spectra were taken on a Nicolet-Impact 400D spectrophotometer in KBr pellets and reported in cm^{-1}. Melting points were determined using Stuart Scientific SMP2 apparatus and are uncorrected. The microwave system used in these experiments includes the following items: Micro-SYNTH lab station, equipped with a glass door, a dual magnetron system with pyramid shaped diffuser, 1000 W delivered power, exhaust system, magnetic stirrer, 'quality pressure' sensor for flammable organic solvents, and a ATCFO fiber optic system for automatic temperature control. The coercivities (H_c), the saturation magnetizations (M_s) and the remnant magnetizations (M_r) of the samples were measured with a vibrating sample magnetometer (VSM) (Meghnatis Daghigh Kavir Co). TGA curve was obtained with a heating rate of 10 °C/min on a TG 50 Mettler thermogravimetric analyzer in the range 30–600 °C. The TEM images were taken with a Philips CM120 unit operated at 200 kV. A scanning electron microscope (SEM) (Philips XL20), equipped with an EDS detector (EDAX) was used to observe the changes in the size and morphology of the samples. An accelerating voltage of 15 kV was used to obtain the SEM images. X-ray photoelectron spectra (XPS) were recorded on an XPS–Auger Perkin Elmer 8025-BesTec electron spectrometer. This instrument includes an ultra-high vacuum chamber, a hemispherical electron energy analyzer and an X-ray source providing unfiltered $K\alpha$ radiation from its Al anode ($h\nu$ = 1486.6 eV). The pressure of the main spectrometer chamber during data acquisition was maintained at ca. 10^{-7} Pa. The binding energy (*BE*) scale was calibrated by using the peak of adventitious carbon, setting it to 284.5 eV. The accuracy of the *BE* scale was ±0.1 eV. The Pd content of the catalyst was determined by a Jarrell-Ash 1100 ICP instrument.

2.3. Synthesis of SPIONs-bis(NHC)-palladium(OAc)$_2$ (**4**)

In a round bottom flask equipped with mechanical stirrer and condenser, a mixture of SiO_2@Fe_3O_4 (4.03 g) and 3-aminopropyltriethoxysilane (APTS) (5 mL) was refluxed in dry toluene (100 mL) at 100 °C for 24 h. After this time, the magnetite nanoparticles were separated from the reaction mixture by an external permanent magnet, washed with ethanol and Mili-*Q* water several times and dried under vacuum at 60 °C to obtain **1**. For preparation of supported *N*-heterocyclic carbene ligand **3**, to a mixture of **1** (0.50 g) in dry THF (40 mL) at 0 °C, 1,3,5-trichlorotriazine (TCT) (0.25 g) was added and the mixture was stirred at 0 °C for 2 h. After consumption of TCT and producing of **2**, as indicated by TLC, diisopropylethyl amine (1 mL) and *N*-methylimidazole (5 mL) were added to this mixture and refluxed in dry toluene for one day. The residue was separated from the mixture by an external permanent magnet, washed with CH_2Cl_2 and THF for several times and finally dried under vacuum at 60 °C to obtain **3**. The final catalyst nanoparticles were obtained as dark-brown solids by addition of $Pd(OAc)_2$ (101 mg, 0.45 mmol) to a dispersed mixture of **3** (1.01 g) in DMSO (5 mL) under argon atmosphere at room temperature. Next, the mixture was stirred for 4 h at 60 °C and then allowed to proceed for an additional 30 min at 100 °C. The resulting complex was collected by an external permanent magnet and washed with ethanol (3 × 10 mL) to remove the unreacted $Pd(OAc)_2$, and finally dried under air (89% yield upon Pd consumption determined by ICP).

2.4. General procedure for Mizoroki–Heck reaction under thermal conditions and microwave irradiation

In a round-bottomed flask equipped with a condenser and a magnetic stirrer, aryl halide (1 mmol), alkene (1.5 mmol), K_2CO_3 (207 mg, 1.5 mmol) and **4** (0.074 g, 0.002 mol% Pd) in DMF (2 mL) was stirred at 90 °C or exposed to MW irradiation (200 W, 70 °C) under air atmosphere. The progress of the reaction was monitored by TLC (eluent:petroleum ether/ethyl acetate, 4:1). After completion of the reaction, the reaction mixture was cooled to room temperature, CH_2Cl_2 (15 mL) was added and the catalyst was separated by an external magnetic field. The organic layer was washed with water (3 × 10 mL) and dried over anhydrous $MgSO_4$. The product was isolated by chromatography on a short column of silica gel to obtain the corresponding products in to 77–90% yields.

2.5. General procedure for Suzuki–Miyaura reaction at room temperature and under microwave irradiation

In a round-bottomed flask equipped with a condenser and a magnetic stirrer, aryl halide (1.0 mmol), aryl boronic acid (1.1 mmol), K_2CO_3 (207 mg, 1.5 mmol), and **4** (0.074 g, 0.002 mol% Pd) were mixed in DMF-H_2O (1:2 V/V). The mixture was stirred at 50 °C or exposed to microwave irradiation (200 W, 70 °C) under air atmosphere. The progress of the reaction was monitored by TLC (eluent:petroleum ether/ethyl acetate, 4:1). After completion of the reaction, CH_2Cl_2 (15 mL) was added (in the case of the reaction under MW irradiation, the mixture was first cooled to room temperature) and the catalyst was separated by a permanent magnet. The organic phase was washed with H_2O (3 × 10 mL), dried over anhydrous $MgSO_4$, and the solvent was evaporated under reduced pressure. The product was isolated by chromatography on a short column of silica gel to obtain the corresponding products in 80–91% yields.

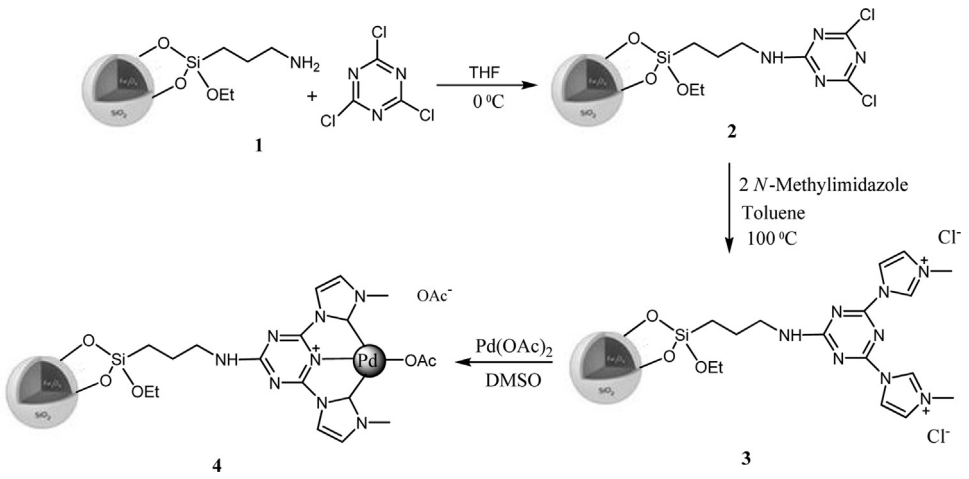

Scheme 1. Synthesis of the catalyst SPIONs-bis(NHC)-palladium(II) diacetate **4**.

3. Result and discussion

3.1. Catalyst preparation and characterization

The preparation of the catalyst follows the steps described in Scheme 1. First, silica-coated magnetite nanoparticles (Fe_3O_4@SiO_2) were selected as support, and subsequently these MNPs were reacted with 3-aminopropyltriethoxysilane (APTS) to obtain the functionalized MNPs **1**. Next, TCT was covalently immobilized onto the surface of the SPIONs by controlling the temperature and then two other chlorides were replaced with two equivalents of *N*-methylimidazole *via* formation of C–N bond between imidazole and triazine parts.

Finally, SPIONs-bis(NHC)-palladium(II) diacetate **4** was prepared by the reaction of $Pd(OAc)_2$ with **3** in DMSO.

The Pd loading of **4**, measured by ICP, showed a value of about 0.27 mmol/g of catalyst. The FT-IR spectrum of **4** showed absorption bands at 584–638 cm^{-1} (Fe–O), 1623 cm^{-1} (C=N), 2927 cm^{-1} (C–H) and 3432 cm^{-1} (N–H stretching vibration).

X-ray photoelectron spectroscopy (XPS) is a powerful tool to investigate the electron properties of the species formed on the surface, such as the electron environment, oxidation state, and the binding energy of the core electron of the metal. Fig. 1 shows the XPS spectrum of **4**. The calibration was performed with the C 1s peak (E_β = 284.5 eV).

As shown in this figure, the peaks at 337.26 ($3d_{5/2}$) and 342.57 eV ($3d_{3/2}$), correspond to Pd with two oxidation states.

The peaks at 335.1 ($3d_{5/2}$) and 340.4 eV ($3d_{3/2}$) indicate that a small portion of Pd is in zero oxidation state [30]. The peaks corresponding to oxygen, carbon, nitrogen, silicon and palladium are also clearly observed in XPS elemental survey of the catalyst.

The thermal stability of **4** was also evaluated by TGA–DTG, and the thermograms are given in the Supplementary material (**F**1). According to these curves, the weight loss below 600 °C is 9.69 and 6%, for **3** and **4**, respectively. So, these results approved that **4** has high thermal stability below 600 °C. This observation can be attributed to the formation of a stable Pd complex. Upon increasing the temperature, first the strong Pd–C and Pd–N bonds should be cleaved which in turns increases the thermal stability of the Pd complex.

The SEM image showed that the shape of Fe_3O_4 nanoparticles is spherical (Supplementary material, **F**2). The presence of the palladium was also confirmed by the EDX detector coupled to the SEM which showed the presence of C, O, Si, Cl, N and Pd (Supplementary material, **F**3).

Transmission electron microscopy (TEM) confirmed the nanometer dimensions of **4** particles (Supplementary material, **F**4). As shown in the particle size histogram, the average size of the magnetic nanoparticles is about 10–11.5 nm.

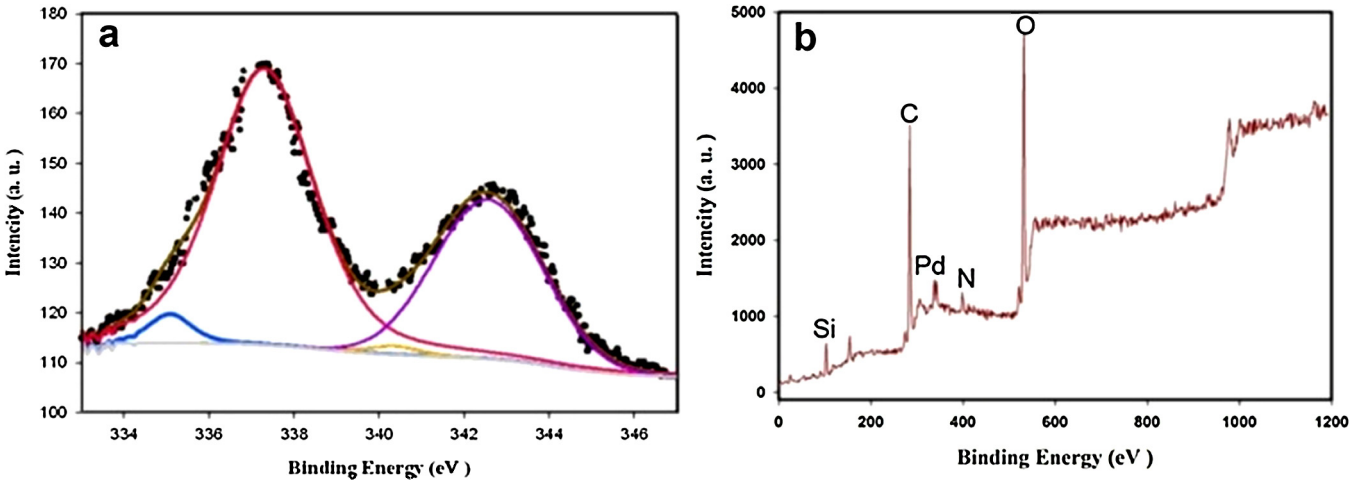

Fig. 1. The XPS spectra of: (a) **4** showing Pd $3d_{5/2}$ and Pd $3d_{3/2}$ binding energies, (b) the elemental survey scan of **4**.

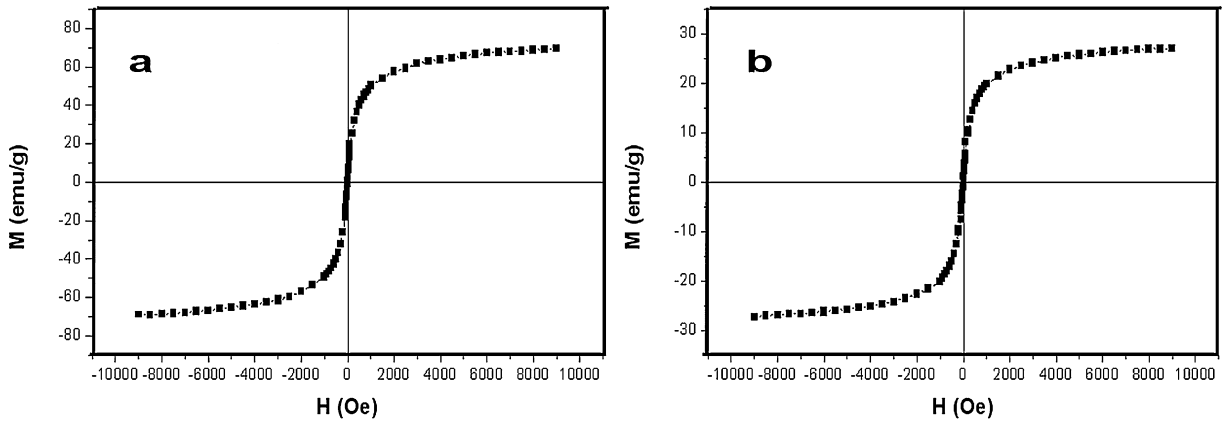

Fig. 2. Room temperature magnetization curves of (a) Fe_3O_4, (b) **4**.

Fig. 2 shows the magnetization curves of Fe_3O_4 and **4**. As shown, the saturation magnetization for Fe_3O_4 is equal to 69.4 emu/g and the magnetization value of **4** was 27.1 emu/g. This investigation proved the super paramagnetic behaviour of the catalyst. Due to the coating of magnetic nanoparticles with silica and also functionalization of silica-encapsulated Fe_3O_4, Ms is found considerably lower than that of the bulk magnetite.

The optimized geometry and molecular orbitals were also investigated at the high level computational method. The calculation was performed with the TURBOMOLE program package, [31,32] making use of the resolution of the identity (RI) approximation for the evaluation of the electron-repulsion integrals. The equilibrium geometry of the ground electronic states (S_0) for SiO_2-APTS-1,3,5-triazin-bis NHC-Pd(II) (compound **4** without consideration of the Fe_3O_4@SiO_2@APTS core) has been determined at the MP2 (Möller–Plesset second order perturbation theory).

The dunning correlation consistent polarized valence dueled zeta basis set (cc-pVDZ) has been used [33]. The optimized geometry of SiO_2-APTS-1,3,5-triazin-bisNHC-Pd(II) is shown in Fig. 3 and some selected geometry parameters on its optimized structure are listed in the Supplementary material.

3.2. Catalytic activity of *4*

After structure characterization of the **4**, its catalytic activity was investigated in the Mizoroki–Heck reaction. In this study, the kind and texture of the catalyst, kind of base, solvent, and reaction temperature were examined in the coupling reaction of iodobenzene (1.0 mmol) and styrene (1.0 mmol), as model reaction (Table 1). As illustrated, the semi-heterogeneous catalyst is much more reactive than the heterogeneous ones.

In the outset, the effectiveness of different solvents such as ethanol, toluene and DMF were examined. DMF appeared to be superior to the others (Table 1, entry 1). Next, the influence of bases in this reaction was investigated. In contrast, using different bases such as NEt_3 or Na_2CO_3 instead of K_2CO_3 evidently gave the lower yields (Table 1, entries 5 and 6).

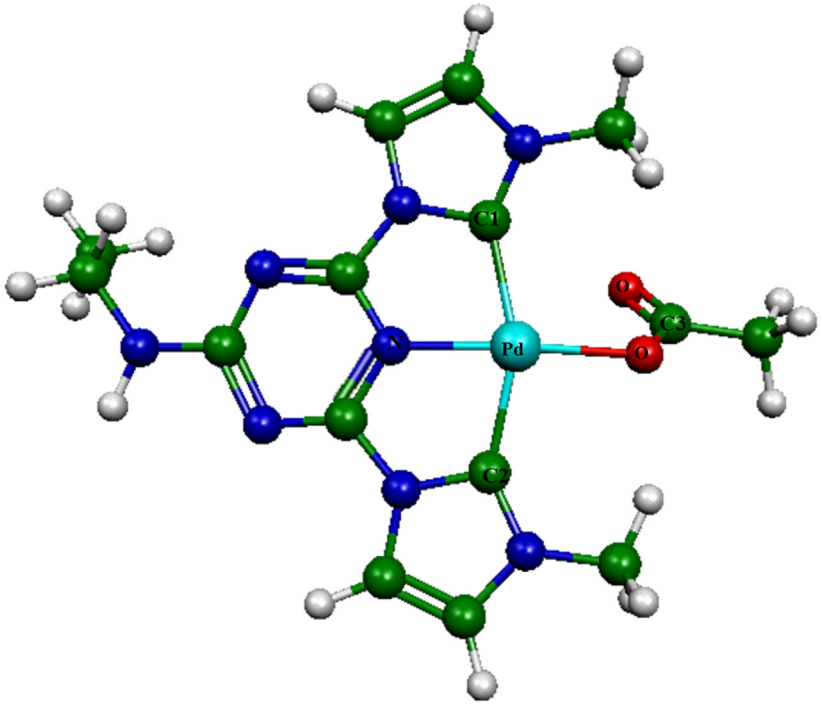

Fig. 3. The optimized geometry of SiO_2-APTS-1,3,5-triazin-bisNHC-Pd(II).

Table 1
Optimization of the reaction of iodobenzene with styrene in the presence of **4**, under thermal condition[a].

Entry	Solvent	Base	Pd [mol%]	T [°C]	t [h]	Yield [%][b]
Solvent effect						
1	DMF	K_2CO_3	0.002	90	2	90
2	Toluene	K_2CO_3	0.002	90	2	60
3	Ethanol	K_2CO_3	0.002	90	3	55
Base effect						
4	DMF	K_2CO_3	0.002	90	2	90
5	DMF	Na_2CO_3	0.002	90	2	50
6	DMF	NEt_3	0.002	90	2	40
Without Pd						
7	DMF	K_2CO_3	–	90	10	–
8	DMF	K_2CO_3	Fe_3O_4	90	8	10
9	DMF	K_2CO_3	nanoSiO_2	90	7	15
Pd loading						
10	DMF	K_2CO_3	0.001	90	4	78
11	DMF	K_2CO_3	0.002	90	2	90
12	DMF	K_2CO_3	0.003	90	3	81
Temperature effect						
13	DMF	K_2CO_3	0.002	80	5	66
14	DMF	K_2CO_3	0.002	90	2	90
15	DMF	K_2CO_3	0.0020	110	3	88

[a] Reaction conditions: iodobenzene (1.0 mmol), styrene (1.5 mmol), catalyst, base (1.5 mmol), solvent (2 mL).
[b] Isolated yield.

Moreover, no reaction occurred in the absence of the catalyst (Table 1, entry 7) and no valuable yield was obtained in the presence of nano-SiO_2, or pure Fe_3O_4 (Table 1, entries 8 and 9). On the other hand, the influence of palladium loading was also investigated. As shown in Table 1, the best result was obtained with 0.002 mol% of catalyst (Table 1, entry 11).

It was also found that the reaction temperature has a great influence on this transformation. The obvious improvement in the conversion (90%) was achieved for the reaction at 90 °C (Table 1, entry 14).

Higher reaction temperature (100–120 °C) gave no better yield but at lower reaction temperature (80 °C), the yield decreased 66% even after long reaction times (Table 2, entries 13 and 15). Therefore, all reactions were carried out at 90 °C in the presence of **4**.

Next, in order to show the influence of microwave irradiation on the Mizoroki–Heck reaction, the results obtained in the reaction of iodobenzene with styrene by conventional heating were compared with the data obtained under microwave irradiation. In the traditional manner an acceptable result was registered after 2 h, but quantitative yield of the corresponding product was obtained under microwave irradiation only after 4 min (Table 2, entry 1).

Table 2
Optimization of the reaction of iodobenzene with styrene in the presence of **4**, under microwave irradiation[a].

Entry	Solvent	Base	Pd [mol%]	Power [W]	T [°C]	Yield [%][b]
Solvent effect						
1	DMF	K_2CO_3	0.002	200	70	96
2	Toluene	K_2CO_3	0.002	200	70	62
3	Ethanol	K_2CO_3	0.002	200	70	57
Base effect						
4	DMF	K_2CO_3	0.002	200	70	96
5	DMF	Na_2CO_3	0.002	200	70	55
6	DMF	NEt_3	0.002	200	70	44
Power effect						
7	DMF	K_2CO_3	0.002	150	50	60
8	DMF	K_2CO_3	0.002	200	70	96
9	DMF	K_2CO_3	0.002	250	80	83

[a] Reaction conditions: mixture of iodobenzene (1.0 mmol), styrene (1.5 mmol), catalyst, base (1.5 mmol) and solvent (2 mL) was irradiated for 4 min.
[b] Isolated yield.

So, this energy source was used as heating system in this transformation. With this achievement we investigated the reaction under microwave irradiation with a temperature controlled program. During irradiation, the temperature was monitored by a fiber optic sensor for controlling the MW power levels. At 70 °C and 200 W, 96% of product was registered after 4 min (Table 2, entry 1). Surprisingly, by increasing the temperature and power up to 80 °C and 250 W, respectively, after 4 min, 83% of the product was isolated (Table 2, entry 9). Notably, lower yields were obtained when the same reaction was carried out with utilizing of lower amount of the catalyst. Under the optimized reaction conditions, several aryl halides were reacted with olefins in the presence of **4** and a large spectrum of cross coupling products was produced through Mizoroki–Heck reaction under microwave irradiation (Table 3). It was generally observed that high to excellent yields of the products were obtained specially in the case of aryl halides bearing electron-donating substituents (Table 3, entry 5–9). In the case of iodobenzene the corresponding products were obtained exclusively with very high turnover frequencies (TOF) (2.2×10^3–2.3×10^4 h^{-1}) (Table 3).

Table 3
Mizoroki–Heck cross coupling of aryl halides and styrene in the presence of **4**.

Entry	$R^1C_6H_4X$	$R^2C_6H_4CH{=}CH_2$	X	Conventional heating[a]			Microwave irradiation[b]		
				Time (h)	Yield (%)[c]	TOF (h^{-1})[d]	Time (min)	Yield (%)[c]	TOF (h^{-1})[d]
1	H	H	I	2	90	2.3×10^4	4	96	6.8×10^5
2	H	4-CH_3	I	8	87	5.4×10^3	7	92	3.8×10^5
3	H	H	Br	7	82	5.8×10^3	4	91	6.5×10^5
4	H	4-CH_3	Br	9	81	4.5×10^3	5	87	5.4×10^5
5	4-CH_3O	4-CH_3	I	6	82	7.0×10^3	5	90	5.6×10^5
6	4-CH_3	H	Br	8	80	5.0×10^3	6	88	4.4×10^5
7	4-CH_3	4-CH_3	Br	9	81	4.5×10^3	8	87	3.3×10^5
8	4-CH_3	H	I	8	78	4.9×10^3	7	83	3.4×10^5
9	4-CH_3	4-CH_3	I	10	77	3.8×10^3	9	81	2.7×10^5
10	4-CH_3CO	H	I	3	89	1.5×10^4	2	93	1.5×10^6
11	4-CH_3CO	4-CH_3	I	5	85	8.5×10^3	4	90	6.4×10^5
12	4-CH_3CO	H	Br	7	82	5.8×10^3	5	88	5.5×10^5
13	4-CH_3CO	4-CH_3	Br	8	84	5.2×10^3	6	90	4.5×10^5
14	4-CHO	H	Br	10	86	4.3×10^3	5	91	5.6×10^5
15	4-F	H	Br	8	87	5.4×10^3	4	92	6.7×10^5
16	4-F	4-CH_3	Br	12	87	7.2×10^3	5	90	5.4×10^5

[a] Reactions were carried out under aerobic conditions 1.0 mmol aryl halide, 1.5 mmol styrene in 2 mL of DMF and 1.5 mmol K_2CO_3 in the presence of **4** (0.074 g, containing of 0.002 mol% Pd).
[c] Isolated yield.
[b] Applied power: 200 W, 70 °C.
[d] (mol product/mol palladium) (h^{-1}).

Table 4
Optimization of the reaction of iodobenzene with phenylboronic acid in the presence of **4** under thermal condition[a].

Entry	Solvent	Base	Pd [mol%]	T [°C]	t [h]	Yield [%][b]
Solvent effect						
1	DMF	K_2CO_3	0.002	50	3	65
2	H_2O	K_2CO_3	0.002	50	4	50
3	H_2O/DMF[c]	K_2CO_3	0.002	50	2	91
Base effect						
4	H_2O/DMF[c]	K_2CO_3	0.002	50	2	91
5	H_2O/DMF[c]	Na_2CO_3	0.002	50	3	49
6	H_2O/DMF[c]	NEt_3	0.002	50	4	42
Temperature effect						
7	H_2O/DMF[c]	K_2CO_3	0.002	25	5	60
8	H_2O/DMF[c]	K_2CO_3	0.002	50	2	91
9	H_2O/DMF[c]	K_2CO_3	0.002	60	3	87
Pd loading						
10	H_2O/DMF[c]	K_2CO_3	0.001	50	5	70
11	H_2O/DMF[c]	K_2CO_3	0.002	50	2	91
12	H_2O/DMF[c]	K_2CO_3	0.003	50	3	75
Without Pd						
13	H_2O/DMF[c]	K_2CO_3	–	90	7	–
14	H_2O/DMF[c]	K_2CO_3	Fe_3O_4	90	5	15
15	H_2O/DMF[c]	K_2CO_3	nanoSiO_2	90	5	20

[a] Reaction conditions: iodobenzene (1.0 mmol), phenylboronic acid (1.1 mmol), catalyst, base (1.5 mmol) and solvent (2 mL).
[b] Isolated yield.
[c] 2:1 (V/V).

Table 5
Optimization of the reaction of iodobenzene with phenylboronic acid in the presence of **4** under microwave irradiation[a].

Entry	Solvent	Base	Pd [mol%]	Power [W]	T [°C]	Yield [%][b]
Solvent effect						
1	DMF	K_2CO_3	0.002	200	70	58
2	H_2O	K_2CO_3	0.002	200	70	42
3	H_2O/DMF[c]	K_2CO_3	0.002	200	70	95
Base effect						
4	H_2O/DMF[c]	K_2CO_3	0.002	200	70	95
5	H_2O/DMF[c]	Na_2CO_3	0.002	200	70	51
6	H_2O/DMF[c]	NEt_3	0.002	200	70	39
Power effect						
7	H_2O/DMF[c]	K_2CO_3	0.002	150	50	70
8	H_2O/DMF[c]	K_2CO_3	0.002	200	70	95
9	H_2O/DMF[c]	K_2CO_3	0.002	250	80	84

[a] Reaction conditions: mixture of iodobenzene (1.0 mmol), phenylboronic acid (1.1 mmol), catalyst, base (1.5 mmol) and solvent (2 mL) was irradiated for 2 min.
[b] Isolated yield.
[c] 2:1 (V/V).

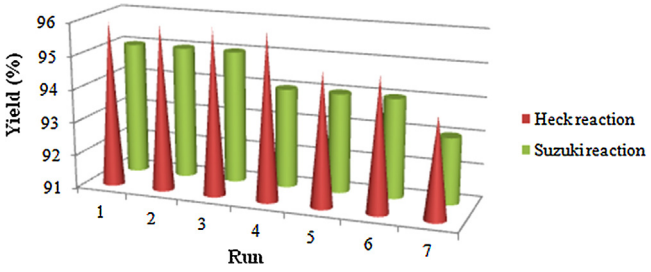

Fig. 4. Reusability of the catalyst.

We also studied the application of this catalyst for the Suzuki–Miyaura reaction. In order to optimize the reaction condition, we studied the reaction of iodobenzene with phenylboronic acid as a model reaction using different bases and solvents (Table 4).

Optimization of the base for the Suzuki reaction was also evaluated by using K_2CO_3, Na_2CO_3, and NEt_3. It was found that K_2CO_3 was the most effective base for this reaction (Table 4, entry 4). Under microwave irradiation, we found that the best yield was obtained at 70 °C and a power of 200 W (Table 5, entry 3). Under the optimized reaction conditions, aryl iodides or aryl bromides, bearing different substituents were converted to their corresponding products in high excellent yields (Table 6).

Compared to the Heck reaction, the Suzuki reaction was performed under milder reaction conditions. The catalyst recycling is important from economical, environmental and industrial points of view. The separation of **4** is a highly simple process, which is achieved by using a permanent magnet. In this manner, the catalyst reusability was checked in the Mizoroki–Heck and Suzuki–Miyaura reactions. At the end of each reaction, the catalyst was separated, washed with ethanol and acetone and reused with fresh substrates in both catalytic systems. As can be seen in Fig. 4, the catalyst was reused several times (seven consecutive runs were checked) without loss of its catalytic activity remarkably.

The amount of Pd leached in both reactions was measured by ICP (Supplementary material). It was observed that only small amounts

Table 6
Suzuki–Miyaura cross coupling of aryl halides and $ArB(OH)_2$ in the presence of **4**.

Entry	$R^1C_6H_4X$	$R^2C_6H_4B(OH)_2$	X	Conventional heating[a]			Microwave irradiation[b]		
				Time (h)	Yield (%)[c]	TOF (h^{-1})[d]	Time (min)	Yield (%)[c]	TOF (h^{-1})[d]
1	H	H	I	4	91	1.1×10^4	2	95	1.6×10^5
2	H	4-CH_3O	I	5	87	8.7×10^3	3	93	9.3×10^5
3	H	H	Br	6	82	6.8×10^3	4	88	6.3×10^5
4	H	4-CH_3O	Br	7	83	5.9×10^3	6	87	4.4×10^5
5	4-CH_3O	H	Br	6	85	7.1×10^3	7	91	3.8×10^5
6	4-CH_3O	4-CH_3O	Br	8	86	5.4×10^3	5	92	5.8×10^5
7	4-CH_3	H	Br	6	88	7.3×10^3	5	91	5.7×10^5
8	4-CN	H	Br	9	81	4.5×10^3	5	87	5.4×10^5
9	4-CH_3CO	H	I	5	85	8.5×10^3	2	90	1.5×10^6
10	4-CH_3CO	4-CH_3O	I	7	84	6.0×10^3	3	90	9.0×10^5
11	4-CH_3	H	I	5	88	8.8×10^4	4	92	6.6×10^5
12	4-CH_3O	H	I	6	89	7.4×10^3	4	93	9.3×10^6
13	4-CH_3O	4-CH_3O	I	5	86	8.6×10^3	5	92	6.6×10^5
14	4-CH_3CO	H	Br	10	84	4.2×10^3	7	89	3.7×10^5
15	4-CH_3CO	4-CH_3O	Br	11	89	4.0×10^3	6	90	4.5×10^5
16	4-CHO	H	Br	14	80	3.6×10^3	5	85	5.3×10^5
17	4-CHO	4-CH_3O	Br	12	84	3.5×10^3	4	86	6.4×10^5

[a] Reactions were carried out under aerobic conditions in 2 mL of mixture of DMF and H_2O (1:2), 1.0 mmol arylhalide,1.1 mmol arylboronic acid and 1.5 mmol K_2CO_3 in the presence of **4** (0.074 g, 0.002 mol% Pd).
[c] Isolated yield.
[b] Applied power: 200 W, 70 °C.
[d] (Mol product/mol palladium) (h^{-1}).

of Pd are leached in the first run and no Pd was detected in the next runs. This can be attributed to the strong attachment of Pd to the NHC ligand.

4. Conclusion

We have demonstrated the synthesis of a new and powerful nanocatalyst which employed in the Mizoroki–Heck and Suzuki–Miyaura reactions, providing very high yields and TOF. The catalyst loading is significantly lower in most cases than previously reported C–C coupling reactions. Easy purification, recyclability and very low Pd leaching are other main characteristic of the process.

We also have successfully developed a general method for the microwave-assisted C–C coupling reactions, providing moderate to high speed, and short reaction times.

Acknowledgment

The authors are grateful to the Center of Excellence of Chemistry of University of Isfahan (CECUI) and also the Research Council of the University of Isfahan for financial support of this work.

Appendix A. Supplementary data

Supplementary data associated with this article can be found, in the online version, at http://dx.doi.org/10.1016/j.molcata.2014.01.001.

References

[1] A.T. Normand, K.J. Cavell, Eur. J. Inorg. Chem. (2008) 2781–2800.
[2] (a) D. Enders, O. Niemeier, A. Henseler, Chem. Rev. 107 (2007) 5606–5655;
(b) S. Díez-Gonzalez, N. Marion, S.P. Nolan, Chem. Rev. 109 (2009) 3612–3672;
(c) P. de Frémont, N. Marion, S.P. Nolan, Coord. Chem. Rev. 253 (2009) 862–892;
(d) S. Budagumpi, R.A. Haque, A.W. Salman, Coord. Chem. Rev. 256 (2012) 1787–1830.
[3] M. Alcarazo, T. Stork, A. Anoop, W. Thiel, A. Fürstner, Angew. Chem. Int. Ed. 49 (2010) 2542–2546.
[4] G. Buscemi, M. Basato, A. Biffis, A. Gennaro, A.A. Isse, M.M. Natile, C. Tubaro, J. Organomet. Chem. 695 (2010) 2359–2365.
[5] M. Poyatos, J.A. Mata, E. Peris, Chem. Rev. 109 (2009) 3677–3707.
[6] O. Schuster, L.R. Yang, H.G. Raubenheimer, M. Albrecht, Chem. Rev. 109 (2009) 3445–3478.
[7] S. Budagumpi, R.A. Haque, A.W. Salman, Coord. Chem. Rev. 256 (2012) 1787–1830.
[8] (a) L.R. Titcomb, S. Caddick, F.G.N. Cloke, D.J. Wilson, D. McKerrecher, Chem. Commun. (2001) 1388–1389;
(b) E.A.B. Kantchev, C.J.O. Brien, M.G. Organ, Angew. Chem. Int. Ed. 46 (2007) 2768–2813;
(c) R.E. Giudici, A.H. Hoveyda, J. Am. Chem. Soc. 129 (2007) 3824–3825.
[9] (a) W.J. Sommer, M. Weck, Coord. Chem. Rev. 251 (2007) 860–873;
(b) N. Debono, A. Labande, E. Manoury, J.C. Daran, R. Poli, Organometallics 29 (2010) 1879–1882;
(c) X. Xu, B. Xu, Y. Li, S. Hong, Organometallics 29 (2010) 6343–6349;
(d) J.D. Blakemore, M.J. Chalkley, J.H. Farnaby, L.M. Guard, N. Hazari, C.D. Incarvito, E.D. Luzik, H.W. Suh, Organometallics 30 (2011) 1818–1829;
(e) Y. Kong, L. Wen, H. Song, S. Xu, M. Yang, B. Liu, B. Wang, Organometallics 30 (2011) 153–159.
[10] Y.H. Chang, Z.Y. Liu, Y.H. Liu, S.M. Peng, J.T. Chen, S.T. Liu, Dalton Trans. 40 (2011) 489–494.
[11] T. Tu, H. Mao, C. Herbert, M.Z. Xu, K.H. Dotz, Chem. Commun. 46 (2010) 7796–7798.
[12] S. Gu, H. Xu, N. Zhang, W. Chen, Chem. Asian J. 5 (2010) 1677–1686.
[13] N. Marion, S.P. Nolan, Acc. Chem. Res. 41 (2008) 1440–1449.
[14] G.C. Fortman, S.P. Nolan, Chem. Soc. Rev. 40 (2011) 5151–5169.
[15] Y. Uozumi, Top. Curr. Chem. 242 (2004) 77–112.
[16] D.Z. Yuan, Q.Y. Zhang, J.B. Dou, Catal. Commun. 11 (2010) 606–610.
[17] M. Choi, D.H. Lee, K. Na, B.W. Yu, R. Ryoo, Angew. Chem. Int. Ed. 48 (2009) 3673–3676.
[18] D.K. Yi, S.S. Lee, J.Y. Ying, Chem. Mater. 18 (2006) 2459–2461.
[19] A.M. Trzeciak, E. Mieczynska, J.J. Ziolkowski, W. Bukowski, A. Bukowska, J. Noworol, J. Okal, New J. Chem. 32 (2008) 1124–1130.
[20] N.T.S. Phan, D.H. Brown, P. Styring, Tetrahedron Lett. 45 (2004) 7915–7919.
[21] N. Gurbuz, I. Ozdemit, B. Cetinkaya, T. Seckin, Appl. Organomet. Chem. 17 (2003) 776–780.
[22] S. Paul, J.H. Clark, J. Mol. Catal. A: Chem. 215 (2004) 107–111.
[23] J.Y. Jung, J.B. Kim, A. Taher, M.J. Jin, Bull. Korean Chem. Soc. 30 (2009) 3082–3084.
[24] K. Bester, A. Bukowska, W. Bukowski, Appl. Catal., A 443–444 (2012) 181–190.
[25] A. Taher, J.B. Kim, J.Y. Jung, W.S. Ahn, M.J. Jin, Synlett (2009) 2477–2482.
[26] P.D. Stevens, J.D. Fan, H.M.R. Gardimalla, M. Yen, Y. Gao, Org. Lett. 7 (2005) 2085–2088.
[27] (a) D. Schaarschmidt, H. Lang, ACS Catal. 1 (2011) 411–416;
(b) S. Moussa, A.R. Siamaki, B.F. Gupton, M.S. El-Shall, ACS Catal. 2 (2012) 145–154;
(c) K.N. Sharma, H. Joshi, V.V. Singh, P. Singh, A.K. Singh, Dalton Trans. 42 (2013) 3908–3918;
(d) Y.Y. Chang, F.E. Hong, Tetrahedron 69 (2013) 2327–2335.
[28] (a) A. Landarani-Isfahani, I. Mohammadpoor-Baltork, V. Mirkhani, A.R. Khosropour, M. Moghadam, S. Tangestaninejad, R. Kia, Adv. Synth. Catal. 335 (2013) 957–972;
(b) M. Shafiee, A.R. Khosropour, I. Mohammadpoor-Baltork, M. Moghadam, S. Tangestaninejad, V. Mirkhani, Catal. Sci. Technol. 2 (2012) 2440–2444.
[29] A. Schatz, M. Hager, O. Reiser, Adv. Funct. Mater. 19 (2009) 2109–2115.
[30] J.F. Moulder, W.F. Stickle, P.E. Sobol, K.D. Bomben, Handbook of X-ray Photoelectron Spectroscopy, Perkin-Elmer Corp., Eden Prairie, MN, 1992, pp. 118.
[31] M. Schreiber, M.R. Silva-Junior, S.P.A. Sauer, W. Thiel, J. Chem. Phys. 128 (2008) 134110–134125.
[32] Turbomole V6.3, a development of the University of Karlsruhe and Forschungazentrum Karlsruhe GmbH, 1989–2007, Turbomole, GmbH, 2007. available from ⟨http://www.turbomole.com⟩.
[33] J.T.H. Dunning, J. Chem. Phys. 90 (1989) 1007–1023.